

Revision 1

The elastic tensor of monoclinic alkali feldspars

Naëmi Waeselmann^{a,1}, J. Michael Brown^a, Ross J. Angel^b, Nancy Ross^c, Jing Zhao^c and Werner Kaminsky^d

Corresponding author: Naemi Waeselmann, Department of Earth and Space Sciences, University of Washington, Seattle, Washington, USA. (naemi@magnet.fsu.edu)

^aDepartment of Earth and Space Sciences, University of Washington, Seattle, Washington, USA.

^bDepartment of Geosciences, University of Padova, Padova, Italy.

^cDepartment of Geosciences, Virginia Tech, Blacksburg, Virginia, USA.

^dDepartment of Chemistry, University of Washington, Seattle, Washington, USA.

¹current address: Florida State University, National High Magnetic Field Laboratory, 1800 E.

Paul Dirac Dr. Tallahassee FL. 32311 USA

Manuscript for American Mineralogist Letters: 22-December-2015

2 **Abstract**

3 The full elastic tensors of two K-rich monoclinic alkali feldspars, Or₈₃Ab₁₅ sanidine and
4 Or₉₃Ab₇ orthoclase have been determined by using the Impulse Stimulated Light Scattering
5 technique to measure surface acoustic wave velocities. The new data confirm that alkali feldspars
6 exhibit extreme elastic anisotropy, so the bounds of their isotropic average properties span a
7 wide range. The measured adiabatic moduli are, for Or₈₃ and Or₉₃ respectively, $K(\text{Reuss}) =$
8 $54.7(7), 54.5(5)$ GPa, $K(\text{Voigt}) = 62.9(1.1), 64.4(0.6)$ GPa, $G(\text{Reuss}) = 24.1(1), 24.5(1)$ GPa and
9 $G(\text{Voigt}) = 36.1(5), 36.1(7)$ GPa. The small differences in moduli between the samples suggests
10 that variations in composition and in state of Al,Si order only have minor effects on the average
11 elastic properties of K-rich feldspars. The new measurements confirm that the earliest
12 determinations of elastic wave velocities of alkali feldspars, widely used to calculate wave
13 velocities in rocks, resulted in velocities systematically and significantly too slow by 10% or
14 more.

15

16 **Introduction**

17 To be able to understand and interpret the seismic signal from the Earth in terms of phase
18 stabilities, and to obtain information about fabric, texture and mineralogy from seismic wave
19 speeds, full knowledge of the anisotropic elastic properties of minerals is required. From these,
20 the wave velocities can be determined. For example p -wave velocities are equal to $(c'/\rho)^{1/2}$
21 where c' is the compressional modulus in the wave propagation direction and ρ the density.
22 Full elastic tensors are also required to interpret diffusion in feldspars (e.g. Schäffer et al. 2014),
23 the morphology of microstructures such as perthite exsolution in feldspars (e.g. Williams and
24 Brown 1974) or the orientation and properties of twin walls (e.g. Salje 2015). Elastic properties
25 are also estimated to contribute to about 50% of the free energy change of displacive structural
26 phase transitions in feldspars (Carpenter and Salje 1994, 1998). An invariant of the full elastic
27 tensor is the bulk modulus, required to define the volume variation with pressure and thus the
28 thermodynamic stability of minerals.

29 Feldspars constitute the most volumetrically important constituent of the Earth's crust, and alkali
30 feldspars are important in deep subduction and high-pressure metamorphism. Yet, the most
31 widely-used elastic data for K-rich alkali feldspars continues to be that of Ryzhova and
32 Aleksandrov (1965), obtained by measurements of ultrasonic wave velocities in pseudo-single
33 crystals of perthites, an intergrowth of albite and K-feldspar, at room conditions. Not only are
34 these velocity data therefore not representative of a single-phase K-rich feldspar, but in-situ high-
35 pressure wave velocity measurements on similar feldspars showed that the room-pressure
36 measurements of Ryzhova and Aleksandrov (1965) yielded p -wave velocities that are
37 systematically slow by between 10 and 30% (Simmons 1964; Christensen 1966). This
38 discrepancy was attributed to the crystals containing cleavage partings and other defects which

39 are open at room pressure and only closed under several kbar of external pressure. This was
40 confirmed by the determination of the full elastic tensor of a gem-quality crystal of monoclinic
41 Or_{89} sandine by ultrasonic resonance measurements (Haussühl 1993) which yielded significantly
42 stiffer values of the individual moduli than those of Ryzhova and Aleksandrov (1965),
43 corresponding to higher wave velocities. Further, the compliances s_{ij} of Haussühl (1993) yield a
44 value of the Reuss bulk modulus $K_R = 55.7$ GPa in reasonable agreement with values of 52(1)
45 and 57(1) GPa determined from two K-rich sanidines by single crystal diffraction (Angel 1994),
46 and significantly higher than the range of $K_R = 39$ to 51 GPa from Ryzhova and Aleksandrov
47 (1965). The single crystal elastic moduli of albite reported by Ryzhova and Aleksandrov (1965)
48 were also shown to be too soft (Brown et al 2006) who also demonstrated that their data
49 acquisition scheme was actually insufficient to determine all 13 independent elastic tensor
50 components of monoclinic crystals.

51 Thus, the only previously published data for the full elastic tensor of K-rich feldspars that is not
52 known to be problematic is the determination by Haussühl (1993). We have therefore undertaken
53 a determination of the full elastic tensors of two additional well-characterized monoclinic K-rich
54 feldspars with differing states of Al,Si order, and differing compositions. Together with the
55 results from Haussühl (1993) they provide a first indication of the possible effects of
56 composition and state of order on the elastic properties of K-rich feldspars and, in combination
57 with the elastic tensor of albite (Brown et al., 2006), an indication of the total variability of
58 elastic properties across the entire alkali feldspar join.

59

60 **Samples and methods**

61 The two current samples (H002 and H003) were provided by J. Schlüter from the collection of
62 the University of Hamburg, Germany. Sample H002 is a natural sanidine of approximate
63 composition $\text{Or}_{83}\text{Ab}_{15}$ with 1.8mol% celsian and 0.5% Sr-feldspar components, H003 is a
64 natural orthoclase of composition $\text{Or}_{93}\text{Ab}_7$ without additional components (Angel et al. 2013).
65 Single-crystal structure refinements (Angel et al. 2013) indicate that H002 sanidine has a more
66 disordered Al,Si distribution than H003 orthoclase, as calculated by the method of Kroll and
67 Ribbe (1983) from the mean tetrahedral bond lengths. In H002, the Al occupancy of the T1 site
68 is calculated as 0.31, whereas it is 0.38 for the orthoclase. The diffraction pattern of H003 also
69 includes the strong diffuse scattering typical of orthoclases and indicates that the local short-
70 range order of Al and Si is higher than indicated by the average from structure refinements (e.g.
71 Pleger 1996; Sanchez-Munoz et al. 1998). Both samples are metrically monoclinic. Densities
72 were determined from the measured compositions and the unit-cell volumes determined by X-ray
73 diffraction (Angel et al., 2013).

74 Surface elastic wave velocities were measured on several different sections of both samples by
75 impulse stimulated light scattering (ISLS) (Abramson et al. 1999). Crystals were oriented on a
76 four-circle X-ray diffractometer and glued to a glass slide while still attached to the goniometer
77 to maintain the orientation. The crystals were then potted in epoxy and ground using 0.25 μm
78 diamond powder for finishing. An aluminum film ~40 nm thick was applied to the surface to
79 allow the coupling of the incident laser energy to the crystal surface and thus the generation of
80 the surface waves. The aluminum film alters surface wave velocities by about 0.1%; this
81 systematic effect is included in the data analysis (Brown et al. 2006). Nine crystals were
82 prepared for H002 and 8 crystals for H003 and the surface wave velocities were measured on
83 each crystal slice in all directions from 0° to 180° (see supplementary material) using steps of 10°

84 (*n.b.* the data from 180° to 360° is identical to the one from 0° to 180°) within the surface (Brown
85 et al. 2006). The elastic moduli reported in table 1 were determined from the measured surface
86 wave velocities through non-linear parameter optimization, using both "Levenberg-Marquardt"
87 and "Nelder-Mead simplex" methods (Brown n.d.). Since the diagonal (e.g. c_{11}) and off-diagonal
88 (e.g. c_{12}) moduli enter into the calculation of surface wave velocities as differences (Brown et al
89 2006), the optimization was further constrained by use of the linear compressibilities
90 $\beta_i = s_{i1} + s_{i2} + s_{i3}$ determined by fitting the unit-cell parameter variation of the same samples at
91 high pressures were measured at Virginia Tech (N.L. Ross, personal communication) by single-
92 crystal X-ray diffraction. The difference between isothermal elasticity (as determined under
93 hydrostatic compression) and adiabatic elasticity (surface wave velocities) is controlled by the
94 factor $(1+\alpha\gamma T)$ where α is thermal expansivity and γ is the Grüneisen parameter. In the case of
95 feldspars near room temperature, the factor $(1+\alpha\gamma T)$ is, within experimental uncertainty, equal to
96 1 (Tribaudino et al. 2011). Thus, the difference between adiabatic and isothermal moduli and
97 compliances is assumed negligible. As for the previous measurement of albite elasticity (Brown
98 et al., 2006) the elastic moduli are described with respect to a Cartesian axial system whose
99 alignment with respect to the non-orthogonal monoclinic crystal axes is $\mathbf{Y} // \mathbf{b}^*$, $\mathbf{Z} // \mathbf{c}$, and $\mathbf{X} // \mathbf{Y} \times$
100 \mathbf{Z} . For the monoclinic samples described in this paper this puts $\mathbf{X} // \mathbf{a}^*$, $\mathbf{Y} // \mathbf{b}$, and $\mathbf{Z} // \mathbf{c}$.

101 **Results**

102 *Anisotropic Behavior*

103 In Table 1 individual moduli (c_{ij}) and components of compressibility, β_i ($i=1-5$) for the alkali
104 feldspars are listed in order of increasing potassium from the pure sodium end-member albite on
105 the left to Or₉₃ on the right. The uniquely triclinic moduli of albite are not listed. In the case of

106 albite, H002 and H003, values for β_1 were independently constrained by the X-ray high-pressure
107 measurements. In the case of Or₈₉, they are derived from the reported elastic moduli. The
108 resulting isotropic moduli and estimated compressional and transverse wave velocities in a
109 random aggregate of the minerals are given at the bottom of the table.

110 The elastic moduli for Or₈₉ reported in Haussühl (1993) indicate that the *a*-axis is the most
111 compressible direction and that the stiffest direction is rotated by 26° towards *a** from the *c*-axis.
112 In addition, the tensor values for thermal expansivity in that study indicate that the *a*-axis has the
113 highest thermal expansivity. Such results are in conflict with all recent studies showing that
114 extrema in elasticity and thermal expansivity for feldspars are closely aligned with *a** and *c*. The
115 elastic moduli listed in Table 1 for Haussühl (1993) have been rotated under the assumption that
116 they were based on a coordinate system with X parallel to the *a*-axis (the coordinate system used
117 in the pioneering work by Ryzhova and Aleksandrov (1965)). That the rotated values are in
118 agreement with the present study provides support for the supposition that the coordinate system
119 used by Haussühl (1993) was that of Ryzhova and Aleksandrov (1965). The alternative
120 assumption, that the coordinate system was correctly described, leads to two equally implausible
121 conclusions: that all recent analyses are wrong or that properties of entirely different materials
122 are being investigated.

123 The elastic moduli show only modest variations across the compositional range and the three
124 potassium-containing feldspars are remarkably similar (see table 1). While the elasticity of albite
125 approximates uniaxial symmetry with $c_{22} \sim c_{33}$ and $c_{12} \sim c_{13}$, the elasticity of the potassium-rich
126 samples is triaxial with $c_{22} > c_{33}$ and $c_{12} > c_{13}$.

127 In figure 1 predicted quasi-longitudinal and quasi-transverse velocities for albite and Or₉₃ are
128 shown in three planes associated with the coordinate system. Velocities for the Or₈₃ and Or₈₉

129 sanidine samples appear identical at the scale of these plots. The high degree of anisotropy
130 previously reported for albite is maintained across the potassium-bearing samples. The degree of
131 anisotropy exhibited by these feldspars is similar to that found in layered structures such as
132 micas (e.g. McNeil and Grimsditch 1993) or portlandite (Speziale et al. 2008). In all samples, the
133 longitudinal velocities are near 8 km/s along both the Y-axis (parallel to crystal *b*-axis) and the
134 Z-axis (parallel to the *c*-axis). The lowest longitudinal velocities (near 5.5 km/s) appear parallel
135 to the X-direction (*a** direction). Quasi-transverse velocities range from slightly more than 2
136 km/s in the X-Y plane to between 5 and 6 km/s in the Y-Z plane. In the Y-Z plane, the quasi-
137 longitudinal and quasi-transverse modes become nearly degenerate between the *c*-axis and the *b*-
138 axis. The quasi-transverse velocities show little directional dependence in the X-Y plane with the
139 slowest velocities just above 2 km/s. Only subtle differences in the patterns of anisotropy are
140 apparent between the albite and orthoclase samples.

141 *Isotropic average properties*

142 For crystals of less than cubic symmetry the two bounding values of the bulk modulus, the Reuss
143 and Voigt bulk moduli, correspond to the stiffness of the single crystal under respectively
144 uniform hydrostatic stress and uniform strain. By definition, the Reuss bulk modulus is identical
145 to the bulk modulus determined in hydrostatic compression measurements. Similar definitions
146 corresponding to uniform shear stress and uniform shear strain conditions give Reuss and Voigt
147 bounds on the shear moduli (e.g. Newnham 2005). These moduli correspond to the widest
148 possible limits for the elastic properties of an aggregate (Avellaneda and Milton 1989;
149 Avellaneda et al. 1996). The tightest constraints that can be determined without a detailed
150 description of the microstructure of the material are provided by the Hashin-Striktmann bounds
151 (e.g. Brown 2015). Since the Hill average of the Voigt and Reuss moduli (K_{VRH} , G_{VRH}) typically

152 falls within the Hashin-Strikmann bounds, this average provides a convenient estimation for
153 properties of an aggregate rock without preferred orientation and with grains locked together. If
154 the grain boundaries are free to ‘slide’ or relax, for example due to the presence of grain
155 boundary fluids or melt, the average moduli will be reduced towards the Reuss bounds.

156 Our two new determinations of the elastic tensors of K-rich alkali feldspars, together with that of
157 sanidine (Haussühl 1993), show that the variation in their average elastic properties is small, of
158 the order of 1% or less in bulk moduli and 3% in shear moduli (Table 1). The VRH average
159 wave velocities from all three samples are $V_p = 6.25(5) \text{ km s}^{-1}$, and $V_s = 3.4(1) \text{ km s}^{-1}$,
160 significantly faster than the velocities derived from the elastic tensors reported by Ryzhova and
161 Aleksandrov (1965) which correspond to ranges of $V_p = 5.6 - 5.9 \text{ km s}^{-1}$ and $V_s = 3.0 - 3.3 \text{ km s}^{-1}$.
162 Further, the bulk moduli of these three K-rich feldspars are very similar to end-member albite
163 but the K-rich feldspars are significantly softer in shear by 5-6 GPa. This is presumably a
164 consequence of the monoclinic-triclinic phase transition. As a consequence, the average elastic
165 wave velocities of albite are higher, by $\sim 0.15 \text{ km s}^{-1}$ for V_p and $\sim 0.3 \text{ km s}^{-1}$ for V_s (Fig 2).

166 **Implications**

167 The anisotropy of the expansion of alkali feldspars as a result of temperature increase (*i.e.*
168 thermal expansion) or substitution of larger cations such as K^+ for Na^+ , has been explained as
169 arising from a particular pattern of co-operative tilting of relatively rigid tetrahedra within the
170 structure. While many possible combinations of tetrahedral tilts are possible, the single co-
171 operative pattern of tilts that operates is that which maximizes short O-O distances within the
172 structure (Angel et al. 2012, 2013). These tilts make the (100) plane normal the direction of
173 greatest expansion and contraction. The fact that we now observe a remarkably similar
174 anisotropy in the elastic properties of alkali feldspars, suggests that at a crystal-chemical level

175 the same mechanisms of tetrahedral tilting are the dominant response of the structure to applied
176 stress, at least in the low-stress regime of linear elasticity represented by the elastic tensors
177 reported here. Obviously, at elevated pressures the structures will become stiffer in the non-
178 linear elastic regime and one can expect additional mechanisms such as tetrahedral deformation
179 to become more significant.

180 The new data, in combination with that of Haussühl (1993) confirms the conclusion of Simmons
181 (1964) and Christensen (1966) that the original determinations by Ryzhova and Aleksandrov
182 (1965) were affected by open spaces in the samples, which led to their calculated average
183 properties being too soft and thus seismic wave velocities that are significantly and
184 systematically too low. The remaining available data now show that the average elastic
185 properties and wave velocities across the alkali-feldspar join (figure 2) vary little with either
186 composition or state of order. There is certainly less than the 15% difference in bulk modulus
187 between sanidine and orthoclase suggested by Hacker (2003), and significantly less than the 30%
188 difference in bulk moduli across the plagioclase feldspar join from albite to anorthite (Angel
189 2004). While these conclusions concerning average properties of alkali feldspars are robust,
190 further work is required to confirm the details of variation of individual elastic moduli and
191 compliances with composition and state of order.

192 **Acknowledgments**

193 This work was supported by grants from the National Science Foundation to JMB (EAR
194 0711591) and NLR and RJA (EAR-1118691). The samples were kindly provided from the
195 Mineralogical Museum of the University of Hamburg by curator Jochen Schlüter.

196

197 **References:**

- 198 Abramson, E.H., Brown, J.M., and Slutsky, L.J. (1999) Applications of impulsive stimulated
199 scattering in the earth and planetary sciences. *Annual Review of Physical Chemistry*, 50,
200 279–313.
- 201 Angel, R.J. (1994) Feldspars at high pressure. In I. Parsons, Ed., *Feldspars and their reactions* pp.
202 271–312. Kluwer Academic Publishers, Dordrecht.
- 203 Angel, R.J. (2004) Equations of state of plagioclase feldspars. *Contributions to Mineralogy and*
204 *Petrology*, 146, 506–512.
- 205 Angel, R.J., Sochalski-Kolbus, L.M., and Tribaudino, M. (2012) Tilts and tetrahedra: The origin
206 of the anisotropy of feldspars. *American Mineralogist*, 97, 765–778.
- 207 Angel, R.J., Ross, N.L., Zhao, J., Sochalski-Kolbus, L., Krüger, H., and Schmidt, B.U. (2013)
208 Structural controls on the anisotropy of tetrahedral frameworks: the example of monoclinic
209 feldspars. *European Journal of Mineralogy*, 25, 597–614.
- 210 Avellaneda, M., and Milton, G.W. (1989) Optimal bounds on the effective bulk modulus of
211 polycrystals. *SIAM Journal on Applied Mathematics*, 49, 824–837.
- 212 Avellaneda, M., Cherkaev, A.V., Gibiansky, L.V., Milton, G.W., and Rudelson, M. (1996) A
213 complete characterization of the possible bulk and shear moduli of planar polycrystals.
214 *Journal of the Mechanics and Physics of Solids*, 44, 1179–1218.
- 215 Brown, J.M. (2015) Determination of Hashin–Shtrikman bounds on the isotropic effective elastic
216 moduli of polycrystals of any symmetry. *Computers & Geosciences*, 80, 95–99.
- 217 Brown, J.M. (n.d.) Determination of elastic moduli from measured acoustic velocities. (to be
218 submitted).
- 219 Brown, J.M., Abramson, E.H., and Angel, R.J. (2006) Triclinic elastic constants for low albite.
220 *Physics and Chemistry of Minerals*, 33, 256–265.
- 221 Carpenter, M.A., and Salje, E.K.H. (1994) Thermodynamics of nonconvergent cation ordering in
222 minerals: III. Order parameter coupling in potassium feldspar. *American Mineralogist*, 79,
223 1084–1098.
- 224 Carpenter, M.A., and Salje, E.K.H. (1998) Elastic anomalies in minerals due to structural phase
225 transitions. *European Journal of Mineralogy*, 10, 693–812.
- 226 Christensen, N.I. (1966) Compressional wave velocities in single crystals of alkali feldspar at
227 pressures to 10 kilobars. *Journal of Geophysical Research*, 71, 3113–3116.
- 228 Hacker, B.R. (2003) Subduction factory 1. Theoretical mineralogy, densities, seismic wave
229 speeds, and H₂O contents. *Journal of Geophysical Research*, 108, 1–26.
- 230 Haussühl, S. (1993) Thermoelastic properties of beryl, topaz, diaspore, sanidine and periclase.
231 *Zeitschrift für Kristallographie*, 204, 67–76.
- 232 Isaak, D.G., Ohno, I., and Lee, P.C. (2005) The elastic constants of monoclinic single-crystal
233 chrome-diopside to 1,300 K. *Physics and Chemistry of Minerals*, 32, 691–699.
- 234 Kroll, H., and Ribbe, P.H. (1983) Lattice parameters, composition, and Al/Si order in alkali
235 feldspars. In Paul H. Ribbe, Ed., *Feldspar Mineralogy* pp. 57–100. Mineralogical Society of
236 America, Washington D. C.

- 237 McNeil, L.E., and Grimsditch, M. (1993) Elastic moduli of muscovite mica. *Journal of Physics:*
238 *Condensed Matter*, 5, 1681–1690.
- 239 Newnham, R.E. (2005) *Properties of materials*, 378 p. Oxford University Press, England.
- 240 Pleger, S. (1996) Diffuse X-ray scattering of homogeneous potassium-rich low- and high-
241 temperature sanidines. *Zeitschrift für Kristallographie*, 211, 293–298.
- 242 Ryzhova, T. V., and Aleksandrov, K.S. (1965) The elastic properties of potassium-sodium
243 feldspars. *Izvestiya of the Academy of Sciences, USSR*, 89-102, Earth Physics Series,
244 *Physics of the Solid Earth (English translation)*, 1, 53–56.
- 245 Salje, E.K.H. (2015) Tweed, twins, and holes, 100, 343–351.
- 246 Sanchez-Munoz, L., Nistor, L., Van Tendeloo, G., and Sanz, J. (1998) Modulated structures in
247 $KAlSi_3O_8$: a study by high resolution electron microscopy and ^{29}Si MAS-NMR
248 spectroscopy. *Journal of Electron Microscopy*, 47, 17–28.
- 249 Schäffer, A.-K., Jäpel, T., Zaefferer, S., Abart, R., and Rhede, D. (2014) Lattice strain across Na-
250 K interdiffusion fronts in alkali feldspar: an electron back-scatter diffraction study. *Physics*
251 *and Chemistry of Minerals*, 41, 795–804.
- 252 Simmons, G. (1964) Velocity of compressional waves in various minerals at pressures to 10
253 kilobars. *Journal of Geophysical Research*, 69, 1117.
- 254 Speziale, S., Reichmann, H.J., Schilling, F.R., Wenk, H.R., and Monteiro, P.J.M. (2008)
255 Determination of the elastic constants of portlandite by Brillouin spectroscopy. *Cement and*
256 *Concrete Research*, 38, 1148–1153.
- 257 Tribaudino, M., Bruno, M., Nestola, F., Pasqual, D., and Angel, R.J. (2011) Thermoelastic and
258 thermodynamic properties of plagioclase feldspars from thermal expansion measurements.
259 *American Mineralogist*, 96, 992–1002.
- 260 Williams, C., and Brown, W.L. (1974) A coherent elastic model for the determination of the
261 orientation of exsolution boundaries: Application to the feldspars. *Acta Crystallographica*
262 *Section A*, 30, 316–331.
- 263

264 **Table 1:** Elastic properties of alkali feldspars.

	Brown et al. (2006)	H002			Haussühl (1993)	H003		
	Or0Ab100 albite	Or83Ab17 sanidine			Or89Ab11 sanidine	Or93Ab7 orthoclase		
Xray density (g cm ⁻³)	2.623		2.567		2.56		2.555	
[ij]	C _{ij} (GPa)***	2σ	C _{ij} (GPa)	2σ	C _{ij} (GPa)**	2σ*	C _{ij} (GPa)	2σ
11	69.9	0.6	69.3	0.6	68.6	0.8	67.8	0.6
12	34.0	0.7	41.6	1.6	43.6	1.6	40.4	1.0
13	30.8	0.5	24.0	0.6	26.0	1.4	25.0	1.0
15	-2.4	0.1	0.3	0.1	-0.7	1.4	-1.1	0.2
22	183.5	2.7	176.2	5.3	176.8	1.0	181.2	3.5
23	5.5	2.2	14.3	3.2	21.0	2.0	20.6	3.9
25	-7.7	0.7	-9.4	0.6	-12.6	2.0	-12.9	0.6
33	179.5	2.3	160.8	2.3	159.9	1.2	158.4	4.0
35	7.1	0.6	7.1	0.5	6.9	1.4	10.6	0.7
44	24.9	0.1	19.2	0.1	19.3	0.4	21.1	0.1
46	-7.2	0.1	-11.5	0.1	-10.8	0.6	-11.6	0.2
55	26.8	0.2	19.4	0.1	18.0	0.8	19.4	0.1
66	33.5	0.2	33.4	0.2	33.5	0.6	33.1	0.2
Compressibilities*	β(TP a ⁻¹)		β(TP a ⁻¹)		β(TP a ⁻¹)		β(TP a ⁻¹)	
1	11.1		11.4	0.05	11.5		11.8	0.06
2	3.4		2.6	0.12	2.4		2.4	0.03
3	3.6		4.3	0.02	4.0		4.1	0.05
5	1.0		-0.5	0.03	0.5		0.0	0.02
Isotropic properties	(GPa)		(GPa)		(GPa)		(GPa)	
KReuss	55.0		54.7	0.7	55.7		54.5	0.5
KVoigt	63.7		62.9	1.1	65.2		64.4	0.6
KVRH	59.4		58.8		60.4		59.5	
GRReuss	29.8		24.1	0.1	23.6		24.5	0.1
GVoigt	41.2		36.1	0.5	35.1		36.1	0.7
GVRH	35.5		30.1		29.4		30.3	
			Km s⁻¹				Km s⁻¹	
Vs (VRH average)	3.7		3.4		3.4		3.4	
Vp (VRH average)	6.4		6.2		6.2		6.3	

265 *The compressibilities are defined in terms of the elastic compliance matrix as $\beta_i = (s_{1i} + s_{2i} + s_{3i})$.

266 **Albite is triclinic and has 21 independent moduli c_{ij} . Only those allowed to be non-zero under monoclinic symmetry are listed here
267 for comparison with the monoclinic feldspars.

268 ***The elastic moduli reported in Haussühl (1993), have been rotated by 26° - see text. Uncertainties listed are in the original
269 coordinate system with the assumption that $l\sigma$ values rather than 2σ values were reported. This assumption is justified through
270 comparison with uncertainties reported in other papers giving moduli for monoclinic crystals using the same technique (*e.g.* Isaak et
271 al. 2006)

Figures

272 Figure 1. Velocities for albite and Or_{93} shown in three different planes. Light gray circles are
273 velocities of 2, 4, 6, and 8 km/s. Dark curves are velocities of quasi-longitudinal and quasi-
274 transverse elastic waves. The orientations of crystallographic axes are shown.

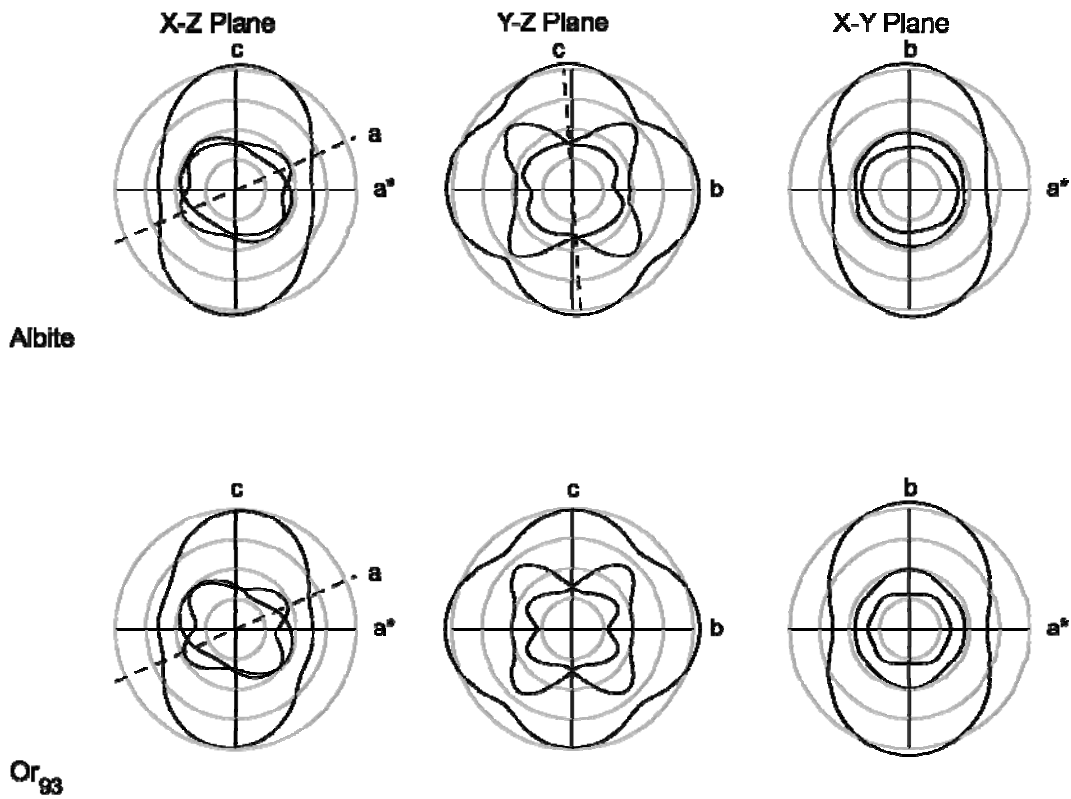
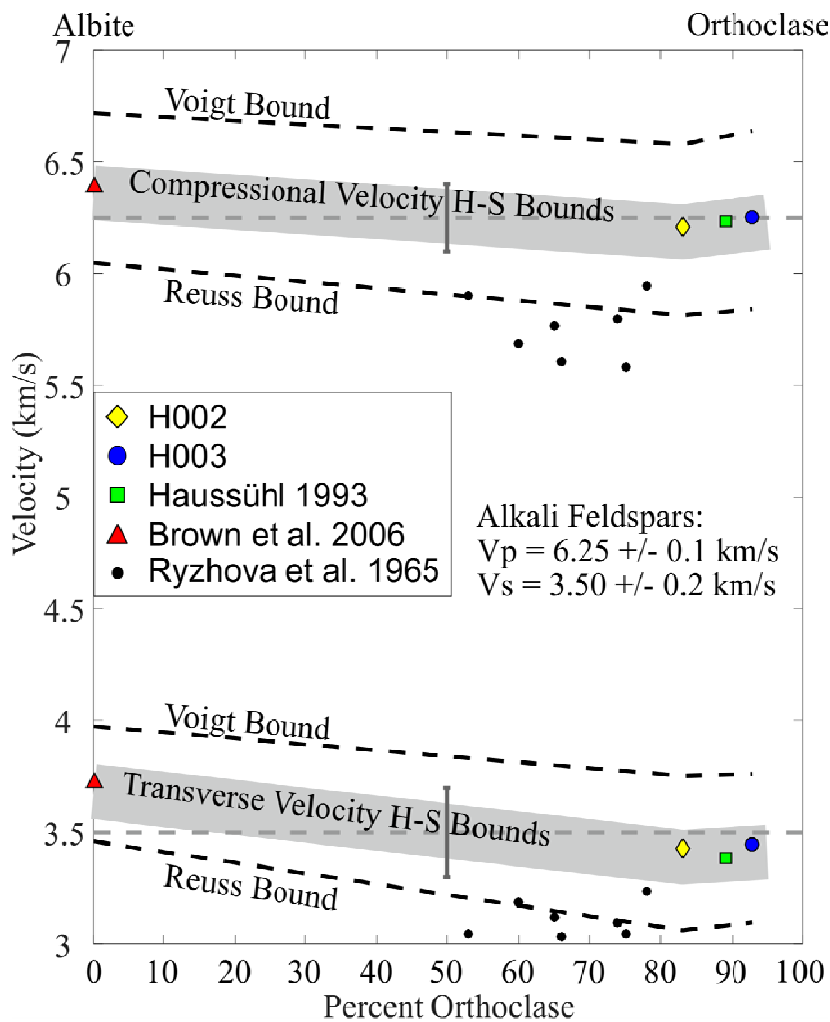
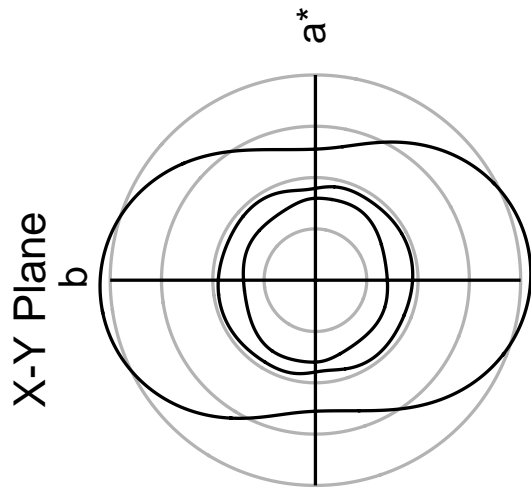
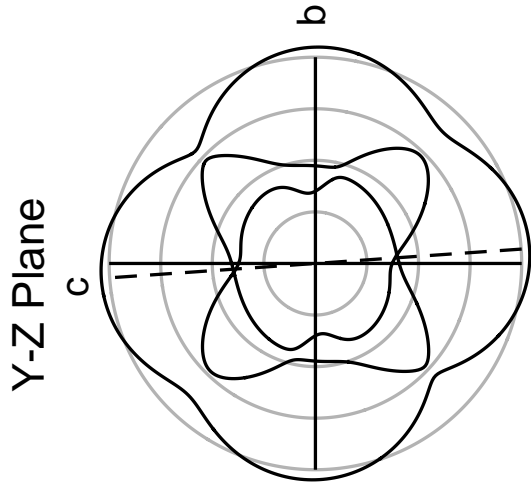
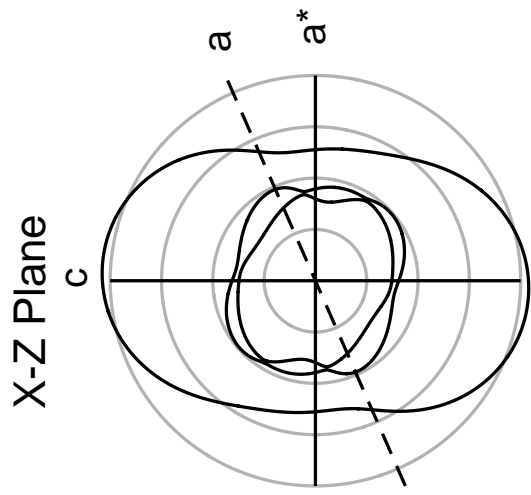


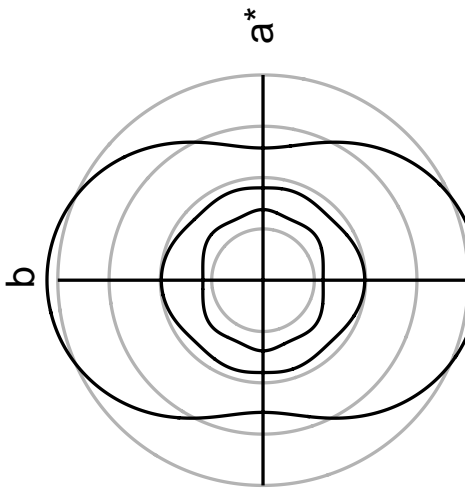
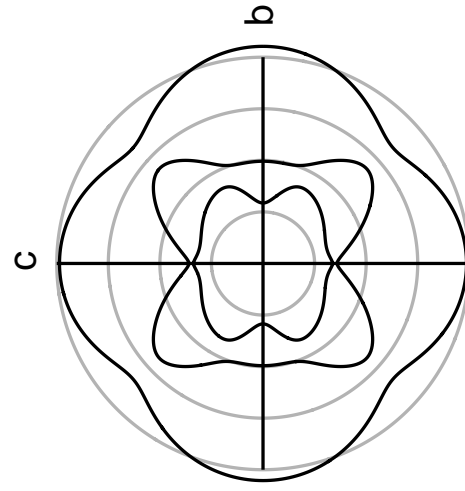
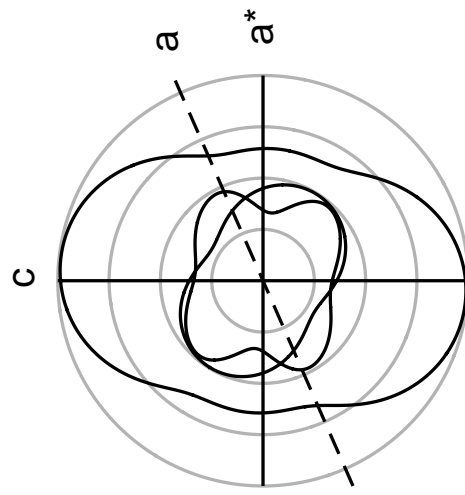
Figure 2: Bounds and averages of the compressional- and transverse wave velocities for alkali feldspars. The Voigt and Reuss bounds are shown by black dashed lines, and the Hashin-Shtrikman bounds as a grey band. The gray dashed line within the Hashin-Shtrikman bounds shows the mean of the Hill averages for alkali feldspars. For comparison with the new data H002 and H003 the data from Haussühl (1993) is given as well as the velocities from Ryzhova and Aleksandrov (1965).



275



Albite



Or₉₃

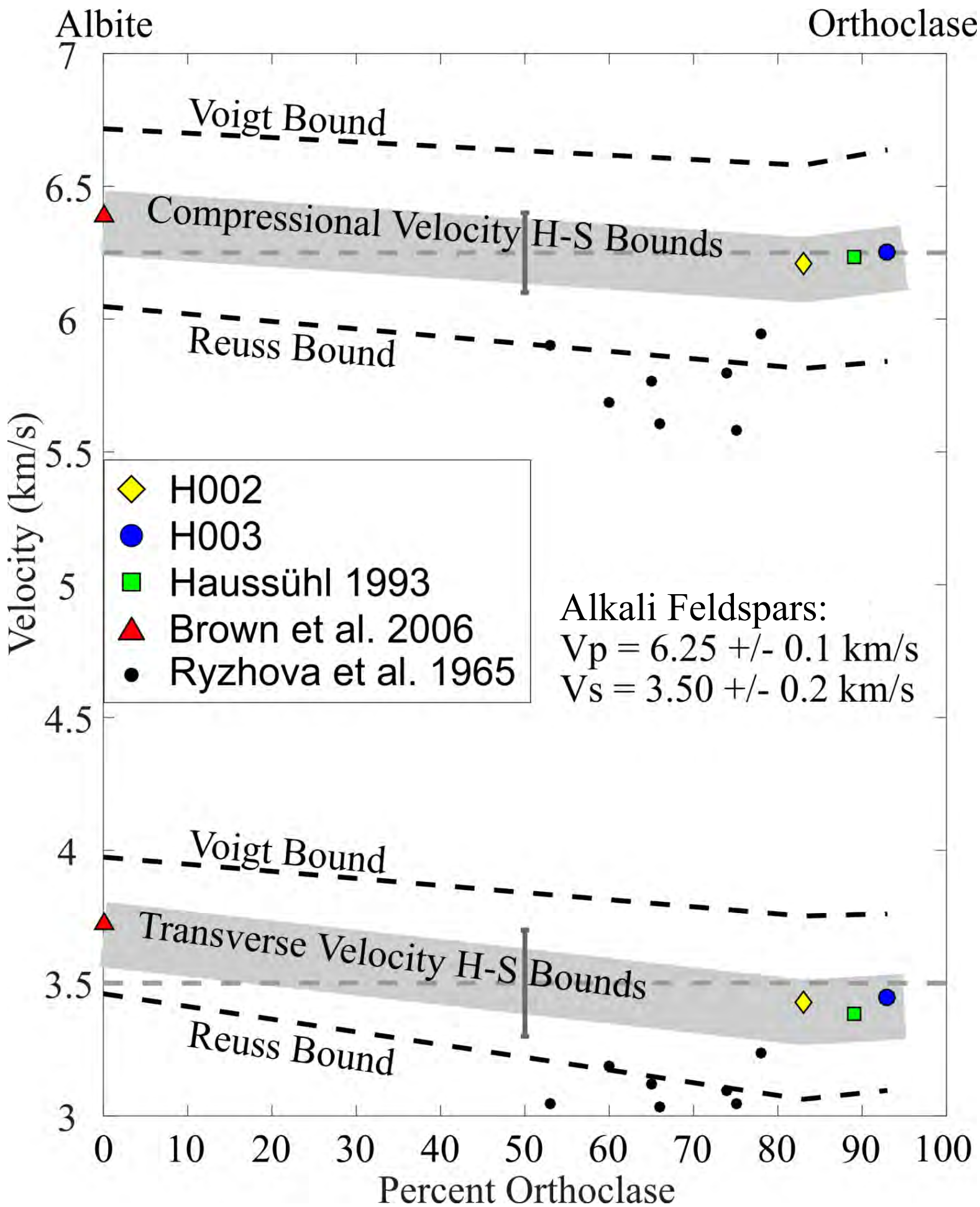


Table 1: Elastic properties of alkali feldspars.

	Brown et al. (2006)	H002		Haussühl (1993)	H003			
	Or0Ab100 albite	Or83Ab17 sanidine		Or89Ab11 sanidine	Or93Ab7 orthoclase			
Xray density (g cm ⁻³)	2.623	2.567		2.56	2.555			
[ij]	C _{ij} (GPa)***	2σ	C _{ij} (GPa)	2σ	C _{ij} (GPa)**	2σ*	C _{ij} (GPa)	2σ
11	69.9	0.6	69.3	0.6	68.6	0.8	67.8	0.6
12	34.0	0.7	41.6	1.6	43.6	1.6	40.4	1.0
13	30.8	0.5	24.0	0.6	26.0	1.4	25.0	1.0
15	-2.4	0.1	0.3	0.1	-0.7	1.4	-1.1	0.2
22	183.5	2.7	176.2	5.3	176.8	1.0	181.2	3.5
23	5.5	2.2	14.3	3.2	21.0	2.0	20.6	3.9
25	-7.7	0.7	-9.4	0.6	-12.6	2.0	-12.9	0.6
33	179.5	2.3	160.8	2.3	159.9	1.2	158.4	4.0
35	7.1	0.6	7.1	0.5	6.9	1.4	10.6	0.7
44	24.9	0.1	19.2	0.1	19.3	0.4	21.1	0.1
46	-7.2	0.1	-11.5	0.1	-10.8	0.6	-11.6	0.2
55	26.8	0.2	19.4	0.1	18.0	0.8	19.4	0.1
66	33.5	0.2	33.4	0.2	33.5	0.6	33.1	0.2
Compressibilities*	β(TP a ⁻¹)		β(TP a ⁻¹)		β(TP a ⁻¹)		β(TP a ⁻¹)	
1	11.1		11.4	0.05	11.5		11.8	0.06
2	3.4		2.6	0.12	2.4		2.4	0.03
3	3.6		4.3	0.02	4.0		4.1	0.05
5	1.0		-0.5	0.03	0.5		0.0	0.02
Isotropic properties	(GPa)		(GPa)		(GPa)		(GPa)	
KReuss	55.0		54.7	0.7	55.7		54.5	0.5
KVoigt	63.7		62.9	1.1	65.2		64.4	0.6
KVRH	59.4		58.8		60.4		59.5	
GREuss	29.8		24.1	0.1	23.6		24.5	0.1
GVoigt	41.2		36.1	0.5	35.1		36.1	0.7
GVRH	35.5		30.1		29.4		30.3	
			Km s⁻¹				Km s⁻¹	
Vs (VRH average)	3.7		3.4		3.4		3.4	
Vp (VRH average)	6.4		6.2		6.2		6.3	

*The compressibilities are defined in terms of the elastic compliance matrix as $\beta_i = (s_{1i} + s_{2i} + s_{3i})$.

**Albite is triclinic and has 21 independent moduli c_{ij} . Only those allowed to be non-zero under monoclinic symmetry are listed here for comparison with the monoclinic feldspars.

***The elastic moduli reported in Haussühl (1993), have been rotated by 26° - see text. Uncertainties listed are in the original coordinate system with the assumption that 1σ values rather than 2σ values were reported. This assumption is justified through comparison with uncertainties reported in other papers giving moduli for monoclinic crystals using the same technique (*e.g.* Isaak et al. 2006)